

Electron Temperature Effect on Plasma Potential for Different Resonant Volumes in Lisa Machine

C. da C. Rapozo, A. Serbêto, A. S. de Assis

Instituto de Física, Universidade Federal Fluminense, 24020, Niterói, RJ, Brasil

and

H. R. T. Silva

Facultad de Ingeniería, Universidad de Tarapaca, 2222, Arica, Chile

Received April 28, 1992; revised manuscript received October 29, 1992

It is shown that the plasma potential drops due to radio frequency interaction in the electron cyclotron resonance (ECR) range of frequency in the linear mirror machine LISA. The plasma has been studied using several diagnostic tools such as Langmuir probe, magnetic probe, Hall probe and Faraday cup. The connection between the potential drop and the anisotropy of the electron temperature is also discussed.

I. Introduction

There have appeared many works on the mechanisms of the electron cyclotron resonance heating (ECRH) in fusion plasma experiments^[1-6]. However, the studies on the anisotropy of the velocity space and the plasma potential drop in localized layer of electron cyclotron are very few^[5,7]. The objective of this work is to investigate the electron cyclotron resonance effect on the plasma potential and its correlation to the anisotropy of the electron temperature in an ECR plasma in LISA machine. Our LISA was constructed at Max-Planck Institut für Plasmaphysik (Garching, Germany), and reassembled at Universidade Federal Fluminense (Niterói, RJ, Brasil).

This paper is organized in the following form: in section II we present the linear mirror machine LISA. In section III we present the experimental results. Discussions and analysis are given in section IV and the conclusion in section V.

II. Experimental Configuration

The physical apparatus used for this experiment is shown in Figure 1 and it was described in previous articles^[5,6]. The helium plasma was produced by a 2.45 GHz magnetron with 800 W, in a stainless steel cylindrical vessel, 17 cm in inner diameter and 255 cm in length. A diffusion vacuum pump provides a pressure of 6×10^{-5} Torr. The axial magnetic field shown in Figure 2 is produced from water cooled coils which are adjusted to produce the desired field profile. Along the longitudinal direction of plasma at $z = 70$ cm we have obtained the resonant magnetic field ($B=875$ Gauss).

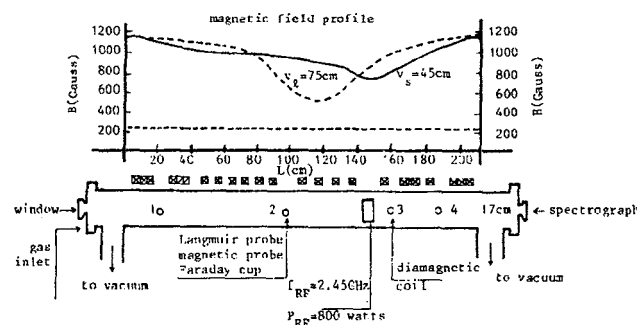


Figure 1: LISA machine.

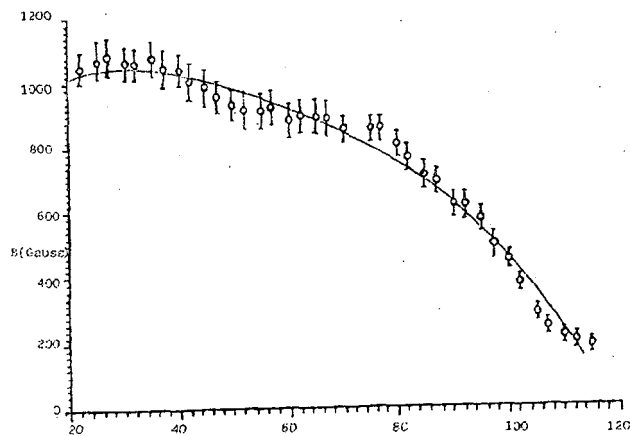


Figure 2: The axial magnetic field profile.

The magnetic field along the axis is not uniform since the waveguide port takes up the space of one coil so that a minimum is formed at that location. This dip helps us to isolate the source from the central mirror region where most of the experimental data are taken. The average electron temperature for large and small resonant volumes is of the order of 40 eV and 30 eV, respectively, and the ion temperature, typically $T_i < 5$ eV, can be considered cold.

Cylindrical disk plane Langmuir probes are used extensively to measure the electron temperature (T_e), the electron plasma density (n_e) and the plasma potential (V_p). Faraday cup is also used to measure T_e and T_i and to check the Langmuir probe measurements. The floating double probes are used to obtain the wave field measurements (E_r , E_θ , E_z). The static magnetic field B_z is measured using a Hall probe. Also the average electron temperature $\langle E_e \rangle$ is obtained spectroscopically. The plasma density is obtained from the ion saturation current.

III. Experimental Results and Analysis

The main objective of this paper was to observe the spatial variation of the plasma and wave parameters in both the radial and axial directions in the resonant zone.

Rapozo et al.^[5] have already studied the radial distribution of plasma pressure, density and temperature for large and small resonant volumes, and the radial distribution of the wave electric field. Those measurements were obtained from gate 2 of LISA device. The fairly uniform radial profiles of T_e and n_e for the radius $r \leq 7.0$ cm are due to the electron-neutral particle collisions ($\nu_{en} \cong .07s^{-1}$). At the point $r = 3.0$ cm, where the microwave power is launched, we observe a maximum electron temperature. The electric field profile is asymmetrical, which from the point of view of the radial distribution, E_θ , seems to correspond to azimuthal wave number $m = 1$ (our E_θ agrees with Figure 5d of ref. 8). From this profile we can see that the point $z = 100$ cm does not correspond to ECR layer, because $B_{res} = 875$ Gauss and this corresponds to B at $z = 70$ cm. The plasma potential is about 90 V at $z = 100$ cm (gate 2). The experimental data above are insufficient to discuss the increase of the electron temperature near the electron cyclotron resonance and the possible plasma potential drop, previously observed by other authors^[7,9].

Figure 3 shows the plasma potential profile as a function of its radius, obtained at gate 3, where there is another strong electron cyclotron resonant layer as a consequence of the nearness of microwave source. Clearly at $r = 3.0$ cm we see a pronounced potential drop at the resonant magnetic field $B_0 = 875$ Gauss when $\omega_{RF} = \omega_{ce}$. Rapozo et al.^[5] have shown that, at this point, the perpendicular and parallel electron temperatures are equal to 50 eV and 35 eV, respectively,

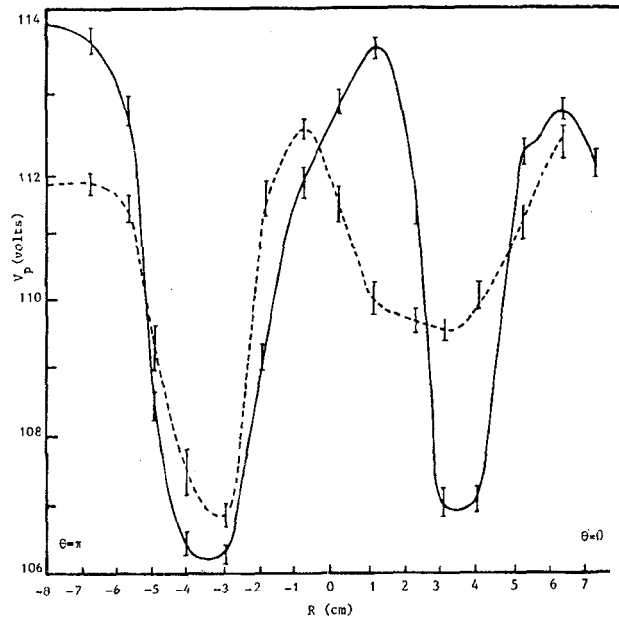


Figure 3: The radial plasma potential profile versus radius for large (full line) and small (dashed line) resonant volumes.

which means that we have a strong anisotropy of the electron temperature during the electron cyclotron resonant heating, characterized by the minimum of the plasma potential.

Figures 4a and 4b show the electric field (E_θ and E_z) profiles for different values of the magnetic field. At $r \cong -2.5$ cm we have a large perpendicular electric field $E_\perp = \sqrt{E_\theta^2 + E_r^2}$ which accelerates the resonant electrons. This shows that the wave absorption occurs at the same radial location where the local temperature is high; the same occurs in the z direction as pointed out in ref. [â]. However for $z > 128$ cm we cannot make measurements of $n(z)$, $T_{e\parallel}(z)$ and $V_p(z)$ due to the distortion produced by the microwave source. For this reason we have to observe the 2nd ECR layer. In order to confirm this remark, besides the associated dips in the plasma potential we have plotted in Figures 5, 6 and 7, $T_{e\parallel}(z)$, $n(z)$ and $V_p(z)$ for values of magnetic coils currents $I_{coil} = 135, 145$ and 150 A, which correspond to $B_0 = 875, 940$ and 970 Gauss, respectively. From these figures we can identify the second ECR layer (where $B = 875$ Gauss) at approximately $z = 70$ cm and observe that the plasma potential is smaller than 80 V when $I_{coil} = 135$ A. Far from this layer the plasma potential can be obtained through a detailed analysis of $T_e(z)$ and $n_e(z)$ via Ohm's law,

$$\eta_{\parallel} J_{\parallel} = E_{\parallel} + \frac{1}{en} \nabla_{\parallel} P_e + 0.71 \frac{k_b}{e} \nabla_{\parallel} T_e, \quad (1)$$

where the last term is the Spitzer's thermoelectric term.

The integration of this equation gives us approxi-

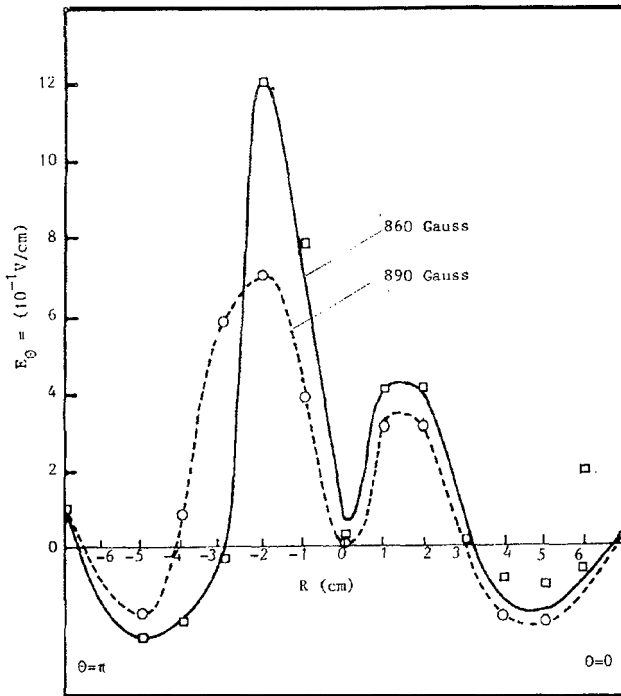


Figure 4a: The azimuthal electric field, E_θ , profile versus radius for different values of magnetic field (860 Gauss and 890 Gauss).

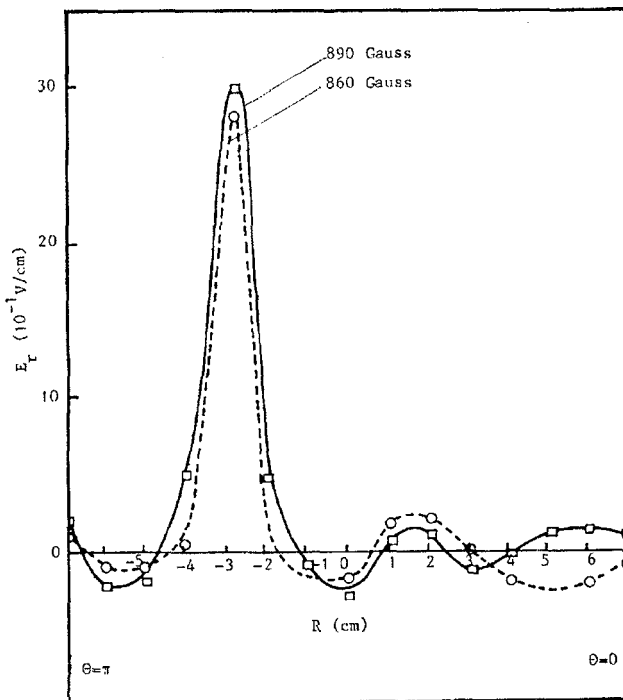


Figure 4b: The radial electric field, E_r , profile versus radius for different values of magnetic field (860 Gauss and 890 Gauss).

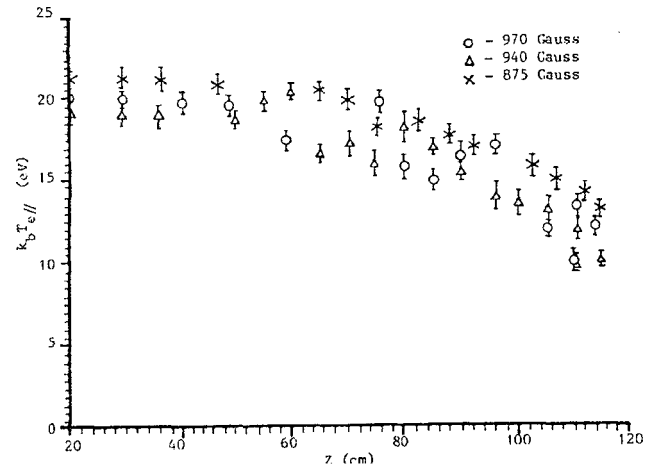


Figure 5: The axial electron temperature profile for different values of magnetic field * 875 Gauss; A 940 Gauss; O 970 Gauss.

mately $V_p \leq 1.7k_b T_{e||}$ when $J_{||} \sim 0$. However, at ECR layer, the correlation between T_e , V , and the wave electric field is more complex because the relativistic effects must be taken into account^[6,11] to show that in this region while the perpendicular "kinetic energy" T is a maximum, the "potential energy" U has a minimum, being^[12]

$$T + U = \text{constant} . \quad (2)$$

Our above results apparently confirm this single particle theory analysis. However, this model is insufficient, from the experimental point of view, due to the plasma density (n_e) and the plasma temperature (T_e).

IV. Discussions and Analysis

The aim of this section is to study the connection among the temperature, the plasma potential and the wave electric field in a ECR plasma heating.

Clearly, in a ECR layer the plasma has a strong anisotropy^[5], so that the energy balance given by refs.[5,13] must be reconsidered. Here, we consider a model where the energy relaxation is given by the electron-neutral collision rate (ν_c), or by stochastic effect (ν_s), with wave power P_w available for the plasma heating, which is related with the components of the electric field E_\perp in the perpendicular, and $E_{||}$, in the longitudinal direction, has a component $P_{w\perp} \approx E_\perp^2$ and $P_{w||} \approx E_{||}^2$, respectively.

The energy balance equations are^[14]

$$n_e k_b \left(\frac{dT_{e||}}{dt} \right) = -(\nu_c + \nu_s) n_e k_b (T_{e\perp} - T_{e||}) + P_{w\perp} - \frac{2T_{e\perp}}{3T_e} (P_{\ell 1} + P_{\ell 2}), \quad (3)$$

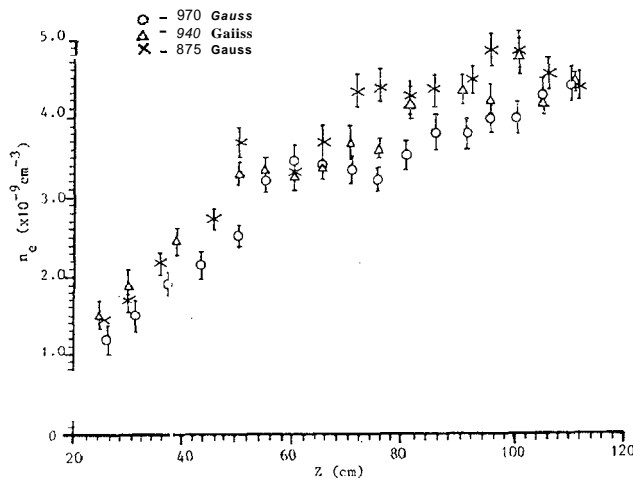


Figure 6: The axial electron density profile for different values of magnetic field * 875 Gauss; A 940 Gauss; O 970 Gauss).

and

$$n_e k_b \left(\frac{dT_{e\parallel}}{dt} \right) = (\nu_c + \nu_w) n_e k_b (T_{e\perp} - T_{e\parallel}) + P_{w\parallel} - \frac{T_{e\parallel}}{3T_e} (P_{\ell 1} + P_{\ell 2}), \quad (4)$$

where $P_{\ell 1}$ and $P_{\ell 2}$ are the power losses due to collisions and the wall current, respectively. The factors $1/3$ and $2/3$ arise from the equipartition of energy to the directions parallel and perpendicular to the magnetic field.

Normally $P_{w\perp} \gg P_{w\parallel}$, such that the energy becomes isotropic and the particle confinement time $\tau_c = n_e k_b T_e / P_w$ is larger than the relaxation time ν^{-1} . Hence, in the steady state situation, considering that $T_{w\perp}$ is constant and $P_{w\parallel} \rightarrow 0$, we have the following anisotropic temperature relations

$$\frac{T_e}{T_{e\parallel}} (T_{e\perp} - T_{e\parallel}) = \frac{P_{w\perp}}{3\nu n_e k_b}, \quad (5)$$

and

$$T_e = \frac{2T_{e\perp} + T_{e\parallel}}{3}, \quad (6)$$

for the average electron temperature, where $P_w = T_{w\perp} = P_{\ell 1} + P_{\ell 2}$ is the power density and $\nu = \nu_{en} + \nu_w$ is the total collision frequency.

These relations show an increase in the electron temperature, when the local electron density n_e decreases. Figure 6 confirms this behavior since the density has a slight dip at the resonance. In Figure 5 we observe the behavior of the parallel temperature $T_{e\parallel}(z)$ which decreases when n_e increases.

The resonant dipping of the plasma potential during the electron cyclotron resonant heating (ECRH) cannot

be explained by the usual theory about the Langmuir probe characteristics, namely^[7,10]

$$\Delta V_p = \left(\frac{\Delta T_e}{2} \right) \ln \left(\frac{M_i}{2\pi m_e} \right), \quad (7)$$

where ΔV_p is the plasma potential drop, M_i is the ion mass and m_e is the electron mass. Here, the variation of the plasma potential should be positive, since the electron temperature at ECR layer is higher than that at the non-resonant region. Therefore, this model is not applicable here. This phenomenon is explained qualitatively^[7,10] by the increase of the ratio $T_{e\perp}/T_{e\parallel}$. However, this approach is non-local since the main agent of ECR, i.e., the electric field of the wave was not considered. To find the relationship among $(T_{e\perp} - T_{e\parallel})$, V_p and the wave power, we will follow the analysis of an ECR plasma made in ref.[3]. The absorbed power density near $\omega_{RF} = \omega_{ce} = eB_0/mc$ is given by

$$P_{RF} = \left(\frac{e^2}{4m_e} \right) |E_\omega|^2 \frac{\sin[(\omega_{ce} - \omega_{RF})t]}{(\omega_{ce} - \omega_{RF})}, \quad (8)$$

where E_ω is the RF resonant field. In the presence of this field, it is conceivable that the increase of the temperature observed at the resonance is a function of E_ω^2 through the potential energy, given by

$$eV_{RF} = \int P_{RF} dt. \quad (9)$$

Then, if we consider the equation

$$V_p = V_{p0} + V_{RF} \cos \omega_{RF} t, \quad (10)$$

we find that the average plasma potential is given by

$$\langle V_p \rangle = V_{p0} - \frac{V_{RF}}{\pi}, \quad (11)$$

where V_{p0} is the value of the plasma potential at off-resonance region where $P_{w\parallel} = 0$.

Combining equations (5) and (11) and considering $T_{e\parallel}/T_{e\perp}$ as a numerical factor, $P_w/\nu = eV_{RF}$ and substituting the numerical value of $n_e k_b$ we obtain

$$\langle V_p \rangle = V_{p0} - \left(\frac{\alpha}{\pi} \right) \left[\frac{k_b (T_{e\perp} - T_{e\parallel})}{e} \right]. \quad (12)$$

where $\alpha > 1$ is a dimensionless numerical factor. This expression gives us a simple relationship between the plasma potential and $(T_{e\perp} - T_{e\parallel})$ at the resonance.

For LISA machine, $a \approx 10$, so we have

$$e[\langle V_p \rangle - V_{p0}] = e\Delta V_p = 3.2k_b (T_{e\perp} - T_{e\parallel}) \text{ (eV)}. \quad (13)$$

Taking $V_{p0} = 120V$, $\langle V_p \rangle = V_{min} = 76V$ at $z = 60$ cm (Figure 7) we have, at the resonance,

$$k_b \Delta T_e = k_b (T_{e\perp} - T_{e\parallel}) = 13.75 \text{ (e)} \quad (14)$$

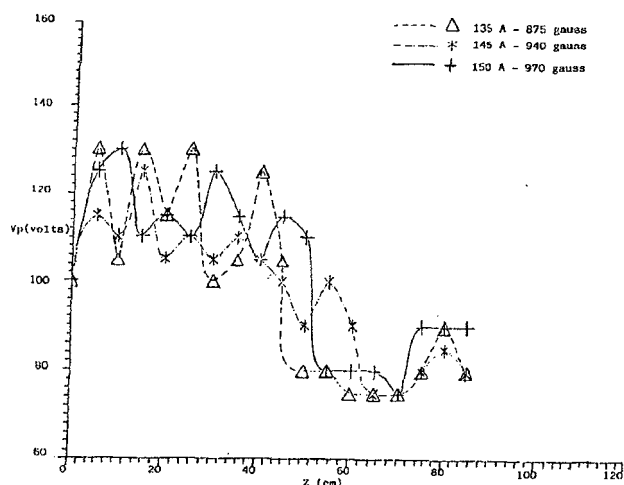


Figure 7: The axial plasma potential profile for different values of magnetic field A 875 Gauss; * 940 Gauss; + 970 Gauss.

which is close to the results obtained in ref. [6] (see Table II, where we have $k_b \Delta T_e = 15$ eV).

Also from Figure 7 we note an interesting shift of the plasma potential drop as a function of the applied magnetic field. $\langle V_p \rangle$ minimum starts at $z = 60$ cm with $k_b \Delta T_e \sim 1$ eV, indicating that the location of ECR is variable; but $e \Delta V_p \sim$ constant for values of B_{dc} from 970 Gauss to 875 Gauss (Table II of ref. [6]), where $k_b \Delta T_{e\parallel} \sim 15$ eV. Considering the typical parameter of LISA machine we have that $T_{e\perp}/T_{e\parallel} \cong 1.3$ without the influence of $P_{\omega\parallel}$. By inspection of equation (3) we can see that $T_{e\perp}/T_{e\parallel}$ increases due to $P_{\omega\parallel}$.

V. Conclusion

In conclusion, we have studied experimentally the plasma potential drop at EC resonance under a low pressure condition; we have shown the connection among the plasma potential, the RF power level and $(T_{e\perp} - T_{e\parallel})$ at the resonance layer.

Our study is very simple and the determination of the plasma potential arises from the condition that the plasma is quasineutral, in the presence of RF wave. Actually, the local potential in the plasma is sensitive to the motion of electrons and ions. In this model, since the ion temperature is smaller than 5 eV, the ion dynamic was not considered. Also, the heating calculation, strictly speaking, should be done in velocity space due to what we have for $T_{e\perp}$ and $T_{e\parallel}$, and the possible formation of a tail in the distribution function was neglected. For these reason, our model can only predict the electron heating up to one order of magnitude.

Acknowledgements

The authors are grateful to Profs. K.H. Tsui and N.L.P. Mansur, the students P.C.M. da Cruz, L.M.V. Sirica and R.P. Menezes, Eng^O H. Teixeira and student M.G. Santos for their helpful contributions to this paper.

This work was supported by the Brazilian agencies: FINEP, CAPES, FAPESP and CNPq.

References

1. A. F. Kuckes, Plasma Physics 10, 367 (1968).
2. J. C. Sprott and P. H. Edmonds, Phys. Fluids 14, 2703 (1971).
3. H. Y. Chang, S. K. Song and Y. J. Kim, Phys. Letters A149, 159 (1990).
4. H. Ikegami, S. Aihara, M. Sasegawa and T. Aikawa, Nucl. Fusion 13, 351 (1971).
5. C. da C. Rapozo, A. S. de Assis, N. L. P. Mansur, L. T. Carneiro and G. H. Cavalcanti, Phys. Scri. 42, 616 (1990).
6. C. da C. Rapozo, A. S. de Assis and J. Busnardo-Neto, Plasma Phys. Controll. Fusion 33, 8 (1991).
7. G. P. Galvão and S. Aihara, Lett. al Nuovo Cimento 33, 140 (1982).
8. L. A. Ferrari, R. J. LaHaye and A. W. McWuade, Phys. Fluids 19, 457 (1976).
9. R. R. Mott, S. W. Lam and J. E. Scharer, IEEE Trans. on Plasma Sci. PS-17, 818 (1989).
10. B. W. Rice and J. E. Scharer, IEEE Trans. on Plasma Sci. PS-14, 17 (1986).
11. K. S. Golovanivsky and V. P. Milantiev, Plasma Phys. Controll. Fusion 16, 5459 (1974).
12. K. S. Golovanivsky, Phys. Lett. A44, 190 (1973).
13. C. da C. Rapozo, K. H. Tsui and A. S. de Assis, Rev. Bras. Fís. 19, 4 (1989).
14. H. Amemiya, H. Oyama, Y. Sakamoto, J. Phys. Soc. Japan. 56, 2401 (1987).
15. B. Chapman, *Glow Discharge Processes* (Wiley, New York, 1980).
16. A. J. Lichtenberg, M. J. Schwartz and M. A. Lieberman, Plasma Phys. Controll. Fusion 13, 89 (1971).
17. C. da C. Rapozo, S. Aihara, U. Carreta and G. Lampis, Il Nuovo Cimento 3D, 1001 (1984).